EJGE

# Mechanical Properties of Ice-Rich Frozen Soil Simulated by Glass Beads Subjected to Cyclic Loading

**Lingshi An [a]*, Xianzhang Ling [a], Yongchang Geng [a], Qionglin Li [b], Feng Zhang [c]**

[a] *School of Civil Engineering, Harbin Institute of Technology, Heilongjiang, Harbin, 150090, China*

[b] *Institute of Engineering Mechanics, China Earthquake Administration, Heilongjiang, Harbin 150080, China*

[c] *School of Transportation Science and Engineering, Harbin Institute of Technology, Heilongjiang, Harbin, 150090, China*

**Corresponding author. e-mail: evanlingshi@163.com*

## ABSTRACT

Since the cyclic loading generated by railways or subways affects the stability of infrastructures constructed in cold regions, it is very important to study the mechanical properties of ice-rich frozen soil subjected to cyclic loading. The soil particles were substituted by glass beads with the aim to avoid the effects of particle shape and weathering degrees. A series of single-stage cyclic triaxial tests under low confining pressure (0.1MPa to 0.3MPa) and temperature (-15℃ to -5℃) were performed to investigate the variation laws of backbone curve and damping ratio of ice-rich frozen soil simulated by glass beads subjected to cyclic loading. In order to study the backbone curve and damping ratio accurately, the determinations of dynamic elastic modulus and damping ratio were showed in detail according to the characteristics of cyclic loading and the original definition of equivalent liner model. The effects of temperature, confining pressure and loading frequency on dynamic elastic modulus and damping ratio were studied. The results showed that temperature had the greatest impact on dynamic elastic modulus and damping ratio. The maximum dynamic modulus gradually increased from 1046MPa to 1832MPa as the loading frequency increased from 2Hz to 6Hz. The lower confining pressure was corresponding to the higher damping ratio for a certain dynamic strain.

KEYWORDS: ice-rich frozen soil; cyclic loading; backbone curve; damping ratio; glass beads

## INTRODUCTION

In cold regions, the cyclic loading is frequently generated by the engineering constructions such as railways, subways or wind turbine towers. The cyclic loading in turn affects the stability of the infrastructures constructed in cold regions. Many investigations show that the mechanical properties of frozen soil subjected to cyclic loading is an important scientific subject (Li, el at., 2013; Viklander, el at., 1998; Zhang, 2012; Simonsen, el at., 2002; Tuğba, el at., 2015; Qi, el at., 2006; Wang, el at., 2007). Unfortunately, most researches were conducted on studying the mechanical characteristics of

the frozen soil with low water content subjected to cyclic loading. Vinson et al. (1978) conducted the cyclic triaxial tests to study the dynamic parameters of frozen clay and the results indicated that the damping ratio increased with the increasing strain amplitude and decreased with the increasing frequency. Ling et al. (2015) pointed out that temperature had the greatest impact on the dynamic shear modulus and damping ratio. Shen et al. (1997) carried out a series of dynamic triaxial compression tests to evaluate the influence of confining pressure on dynamic strength of frozen soil. The conclusion that the dynamic strength increased with the confining pressure first and then decreased with the confining pressure after reached its peak value at some confining pressure was achieved. Xie et al. (2014) found that the dynamic compressive stress-strain curve of frozen soil could be divided approximately into three stages: the elastic stage, plastic stage and softening stage.

Although the area of ice-rich frozen soil accounts for 24% of the world's land area, few investigations have been done on the mechanical properties of ice-rich frozen soil subjected to cyclic loading. Gao et al. (2010) evaluated the dynamic mechanical properties of warm ice-rich frozen clay. The results indicated that the dynamic modulus increased at first and then decreased as the dynamic strain increased when the confining pressure was below 0.5MPa.

It should be pointed out that the previous studies on mechanical properties of ice-rich frozen soil subjected to cyclic loading were conducted under warm temperature (greater than -2℃) and high confining pressure (greater than 0.5MPa). In other words, under low confining pressure and temperature condition, there is some lack of knowledge about the mechanical properties of ice-rich frozen soil subjected to cyclic loading. In addition, the shape and weathering degrees of soil in previous studies were different.

The main objectives of this paper are to (1) substitute glass beads for soil particles in order to avoid the effects of particle shape and weathering degrees; (2) show the determinations of dynamic elastic modulus and damping ratio according to the characteristics of cyclic loading and the original definition of equivalent liner model and (3) study the dynamic elastic modulus and damping ratio of ice-rich frozen soil simulated by glass beads under low confining pressure (0.1MPa to 0.3MPa) and temperature (-15℃ to -5℃) based on the single-stage cyclic triaxial tests.

# LABORATORY TEST PROGRAM

## Materials

The soil particles were substituted by four sizes of smooth glass beads: diameter of 4mm, 5mm, 6mm and 7mm (Fig. 1). The curvature and non-uniformity coefficients of glass beads are 1.028 and 1.4 respectively. The grain size distribution curve of glass beads is presented in Fig. 2.

**Figure 1:** Glass beads

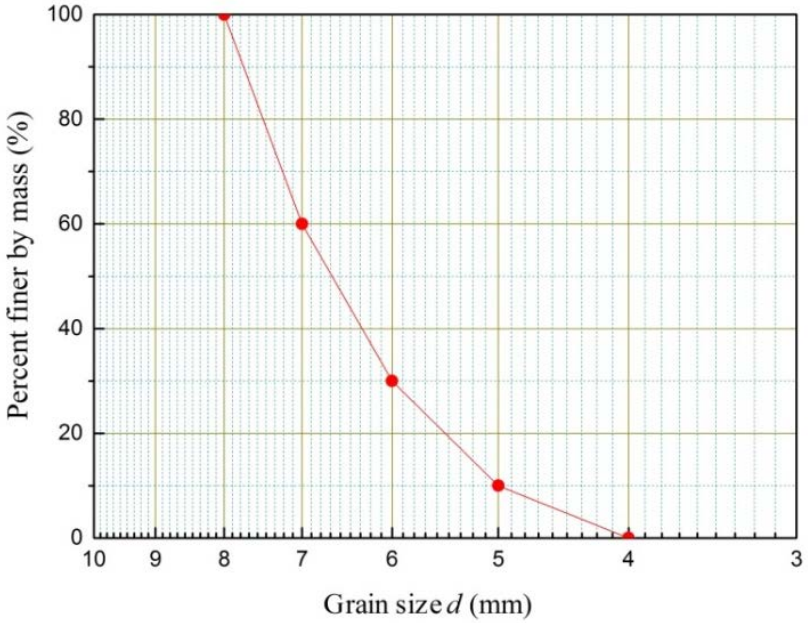


**Figure 2:** Grain size distribution curve of glass beads

## Test devices

The single-stage cyclic triaxial tests were carried out in Heilongjiang Provincial Hydraulic Research Institute. The test device in this experiment is the TWDSZ300 (an electric-hydraulic servo controlled material testing machine) which is equipped with an automatic numerical control system and a data collection system (Fig. 3). The temperature can be controlled by a refrigeration system and temperature sensors to a minimum value of -30℃. The vertical electric-hydraulic servo controlled loading system can perform strain-controlled or stress-controlled tests with a maximum axial force of

100kN, a maximum axial displacement of 85mm and a maximum frequency of 40Hz. The confining pressure can be applied by an anhydrous alcohol pressure piston over the range of 0-30MPa.

**Figure 3:** The cyclic triaxial material testing machine

## Specimens preparation and test conditions

Considering that few attempts have been focused on how to make the frozen glass beads specimens, it is necessary to show some details about the processes of preparing specimens. The procedures of preparing specimens were performed according to the Specification of Soil Test (SL237) and were designed as following: (1) We put a circular flat iron into a plastic cup for preventing damage to the plastic cup when the specimen was compacted. (2) We coated a film of frostproof oil such as aircraft hydraulic oil on the internal surface of the three segment copper molds with a diameter of 39.1mm and height of 80mm. We then attached a flexible thin-film closely to the frostproof oil so as to separate the specimen from the three segment copper molds conveniently. (3) We put the three segment copper molds into the plastic cup. We then put the glass beads into the three segment copper molds in same three layers and each layer was compacted. We thereafter put a circular flat iron was on the top of three segment copper molds. Note that the mass percents of glass beads with the diameter of 4mm, 5mm, 6mm and 7mm were 10%, 20%, 30% and 40% respectively. (4) We filled the plastic cup with water, as shown in Fig. 4 and then we put the plastic cup into an automatic temperature-controlled refrigerator with the temperature of -40℃ to freeze for 12 hours, in which the specimen was frozen quickly to avoid the effect of frost heave, as shown in Fig. 5. (5) We dismantled the three segment copper molds, as shown in Fig. 6 and kept the specimen in an incubator for 12 hours under the target testing temperature so that the specimen had a uniform temperature. (6) We made the specimens in batches to make sure the comparability. Note that the volumetric ice content of the specimens was about 40%.

**Figure 4:** The specimen before freezing

**Figure 5:** The automatic temperature-controlled refrigerator

**Figure 6:** The prepared specimen

Taking the field monitoring results and test apparatus into account, the cyclic loading with the sine-wave form was applied on the specimens only in axial direction and the lateral stress was constant as shown in Fig. 7. The cyclic triaxial tests were performed under single-stage loading instead of multi-stage loading with the aim to study the dynamic elastic modulus accurately. The details of experiment scheme are summarized in Table 1 in detail.

**Table 1:** Cyclic triaxial test conditions

| Specimen | Temperature | Loading frequency | Confining pressure |
|---|---|---|---|
| BZDwd1 | -5℃ | 4Hz | 0.2MPa |
| BZDwd2 | -10℃ | | |
| BZDwd3 | -15℃ | | |
| BZDpl1 | -10℃ | 2Hz | 0.2MPa |
| BZDpl2 | | 4Hz | |
| BZDpl3 | | 6Hz | |
| BZDwy1 | -10℃ | 4Hz | 0.1MPa |
| BZDwy2 | | | 0.2MPa |
| BZDwy3 | | | 0.3MPa |

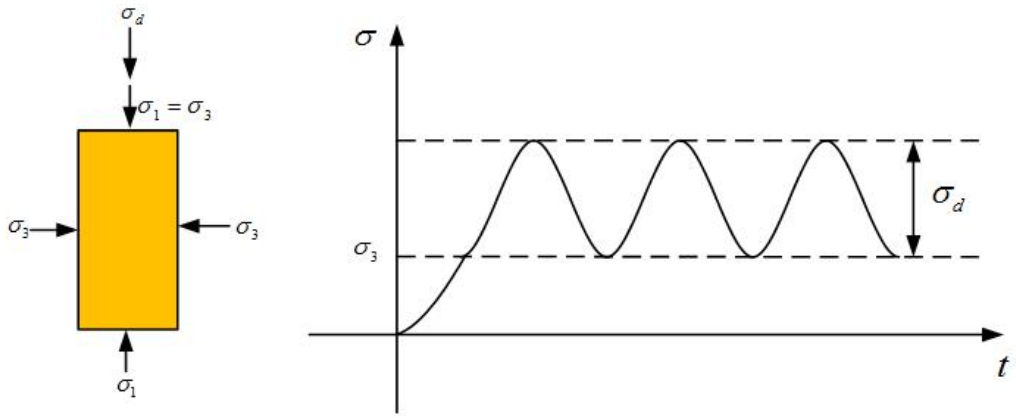


**Figure 7:** Load-on pattern of cyclic loading

## Test results and discussion

*(a) Determinations of dynamic elastic modulus and damping ratio*

Fig. 8 shows the stress-strain curve of ice-rich frozen soil simulated by glass beads subjected to cyclic loading. It can be seen that the hysteresis curve is not a closed cycle due to the accumulation of residual strain. The second loop is chosen as an example to explain the determination of dynamic elastic modulus in detail. The second loop is composed of the loading curve (ABC) and the unloading curve (CDE). Points A and C are the origin and tip of the loop respectively. According to the equivalent linear model, the dynamic elastic modulus is defined as the slope of line AC. The dynamic elastic modulus can be described by Eq. (1):

$$E_d = \frac{\sigma_t - \sigma_o}{\varepsilon_t - \varepsilon_o} = \frac{\sigma_d}{\varepsilon_d} \tag{1}$$

Where $\sigma_o$ and $\sigma_t$ are the dynamic stress of the origin and tip of the hysteresis curve respectively; $\varepsilon_o$ and $\varepsilon_t$ are the dynamic strain of the origin and tip of the hysteresis curve respectively.

The Hardin hyperbolic model is frequently used to describe the relationship between dynamic stress and dynamic strain can be expressed by Eq. (2):

$$\sigma_d = \frac{\varepsilon_d}{a + b\varepsilon_d} \tag{2}$$

Where $a$ and $b$ are the model parameters.

Upon substitution of Eq. (1) into Eq. (2), the dynamic elastic modulus can be can be defined by Eq. (3):

$$E_d = \frac{\sigma_d}{\varepsilon_d} = \frac{1}{a + b\varepsilon_d} \tag{3}$$

Based on Eq. (3), the maximum dynamic elastic modulus $E_{d\max}$ and the ultimate dynamic stress

magnitude $\sigma_{dult}$ can be described by Eq. (4) and Eq. (5) respectively.

$$E_{d\max} = E_d\big|_{\varepsilon_d \to 0} = \frac{1}{a} \tag{4}$$

$$\sigma_{dult} = \sigma_d\big|_{\varepsilon_d \to +\infty} = \frac{1}{b} \tag{5}$$

Upon substitution of Eqs. (4) and (5) into Eq. (3), the dynamic elastic modulus can be written as follows:

$$E_d = \frac{\frac{1}{a}}{1+\left(\frac{b}{a}\right)\varepsilon_d} = \frac{E_{d\max}}{1+\left(\frac{b}{a}\right)\varepsilon_d} \tag{6}$$

Combining Eq. (4) and Eq. (5), the reference shear strain magnitude $\varepsilon_{dr}$ can be expressed by Eq. (7):

$$\varepsilon_{dr} = \frac{\sigma_{dult}}{E_{d\max}} = \frac{a}{b} \tag{7}$$

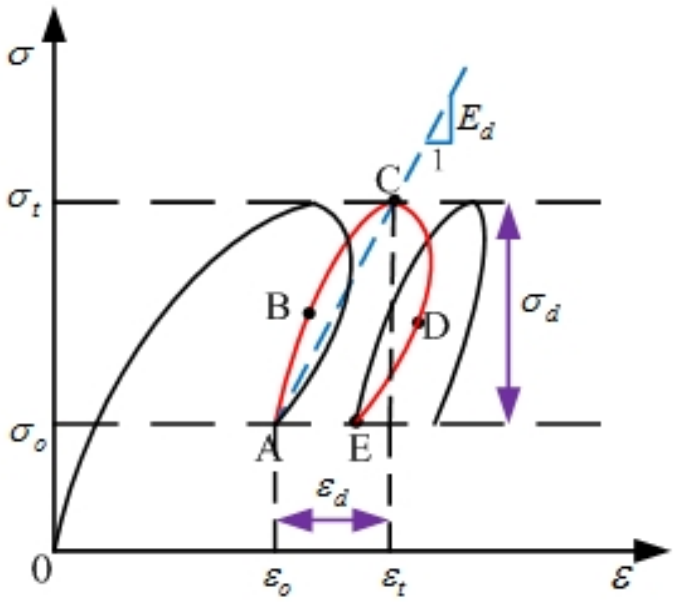


**Figure 8:** Determination of dynamic elastic modulus

The damping ratio describes the energy consumption of ice-rich frozen soil simulated by glass beads subjected to cyclic loading, as shown in Fig. 9 and it can be defined by Eq. (8):

$$\lambda = \frac{1}{4\pi}\frac{\Delta W}{W} \tag{8}$$

Where $\Delta W$ is the area of the loop ABCDE and $W$ is the area of the triangle ACF.

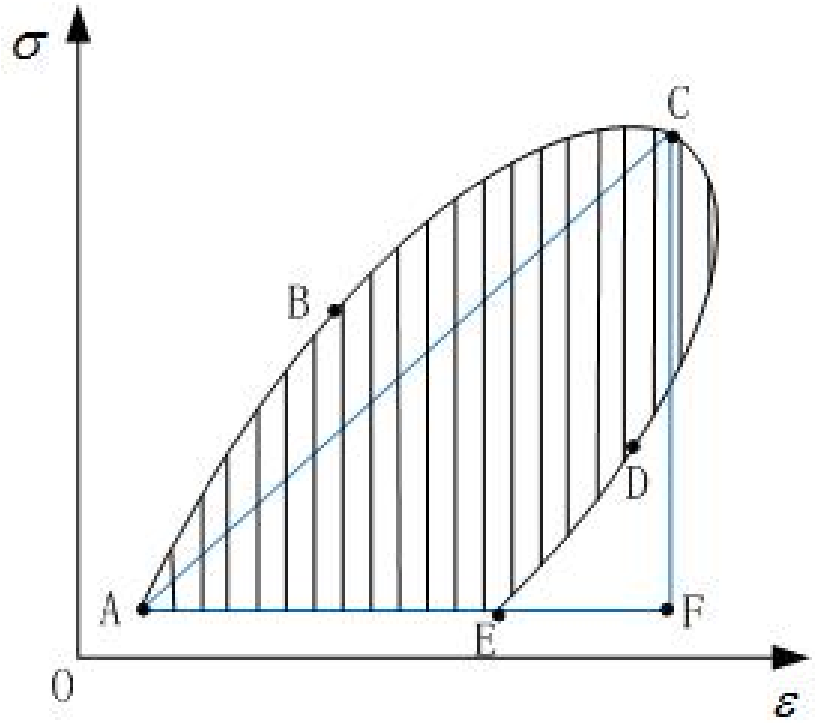


**Figure 9:** Determination of damping ratio

The damping ratio can also be expressed by Eq. (9): (Seed et al., 1984; Seed and Idriss, 1970; Hardin and Drmevich, 1972):

$$\lambda = \lambda_{max}\left(\frac{\varepsilon_d/\varepsilon_{dr}}{1+\varepsilon_d/\varepsilon_{dr}}\right) \tag{9}$$

Where $\lambda_{max}$ is the maximum damping ratio.

*(b) Influence of temperature*

The impacts of temperature on dynamic elastic modulus and damping ratio were studied by three tests under different temperatures (-5℃, -10℃, -15℃). In addition, the confining pressure was 0.2MPa and the loading frequency was 4Hz. The effect of temperature on backbone curve can be indicated by Fig. 10. It is evident that temperature has the greatest impact on backbone curve. The stiffness of the specimen at low temperature is greater than that of the specimen at high temperature. The evolution of maximum dynamic elastic modulus versus temperature is presented in Fig. 11. As shown in Fig. 11, the maximum dynamic elastic modulus decreases from 2439MPa to 781MPa which means a 68 percent decline as the temperature increases from -15℃ to -5℃. The relationship between damping ratio and temperature is presented in Fig. 12. It can be seen that temperature also

has the greatest impact on damping ratio. The damping ratio ranges from 0.19 to 0.35. The possible reason for the phenomena is that the inter-particle bonding strength decreases with the increase of temperature. Furthermore, the unfrozen water which can reduce the inter-particle friction increases with the increasing temperature. The model parameters $a$ and $b$ of Hardin hyperbolic model are listed in Table 2.

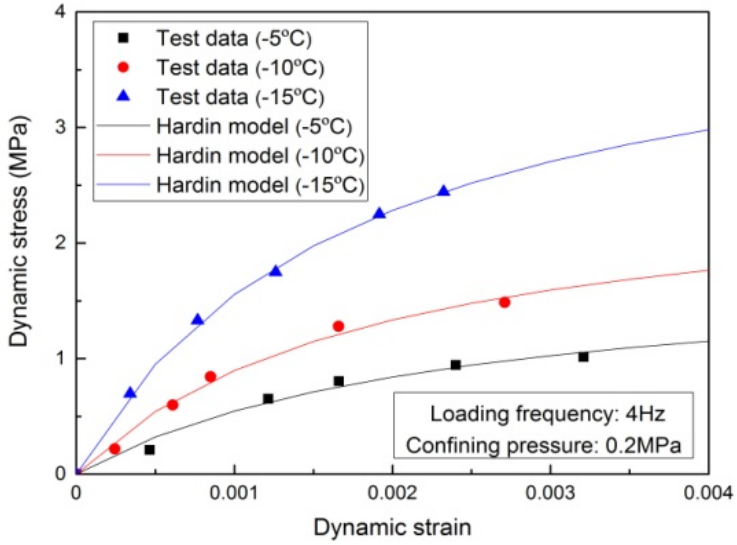


**Figure 10:** Backbone curves under different temperatures

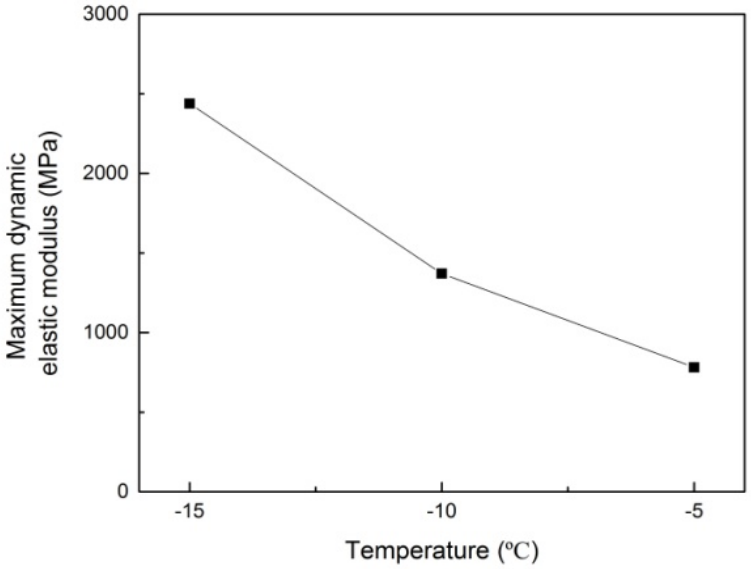


**Figure 11:** The relationship between maximum dynamic elastic modulus and temperature

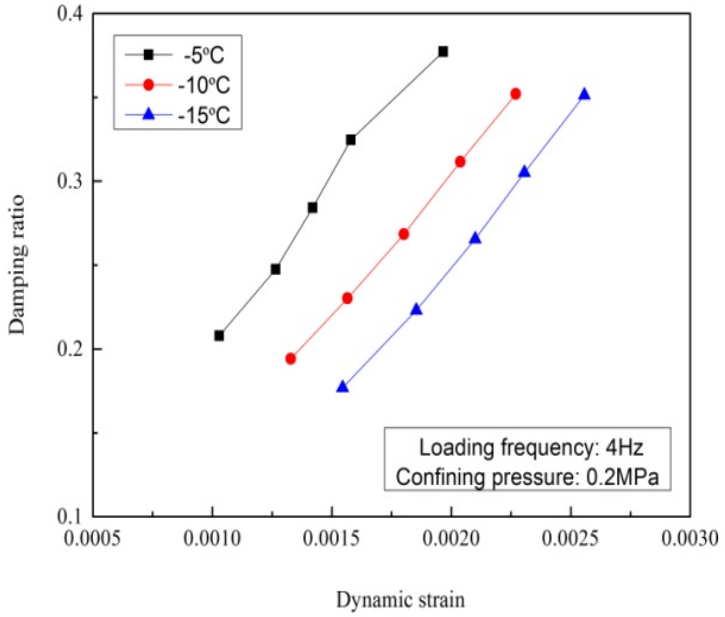


**Figure 12:** Damping ratios under different temperatures

**Table 2**: The model parameters *a* and *b* of Hardin hyperbolic model

| Specimen | *a* | *b* |
|---|---|---|
| BZDwd1 | 0.00128 | 0.54 |
| BZDwd2 | 0.00073 | 0.38 |
| BZDwd3 | 0.00042 | 0.23 |
| BZDpl1 | 0.00095 | 0.37 |
| BZDpl2 | 0.00073 | 0.38 |
| BZDpl3 | 0.00054 | 0.36 |
| BZDwy1 | 0.00081 | 0.41 |
| BZDwy2 | 0.00073 | 0.38 |
| BZDwy3 | 0.00058 | 0.34 |

*(c) Influence of loading frequency*

Three tests with different loading frequencies (2Hz, 4Hz and 6Hz) were carried out to study the impacts of loading frequency on dynamic elastic modulus and damping ratio. In addition, the confining pressure was 0.2MPa and the temperature was -10℃. Fig. 13 shows the backbone curves under various loading frequencies. The dynamic stress tends to increase with the increasing loading frequency for a certain dynamic strain. The relationship between maximum dynamic modulus and loading frequency is shown in Fig. 14. It is obvious that the maximum dynamic modulus gradually increases from 1046MPa to 1832MPa as the loading frequency increases from 2Hz to 6Hz. The effect of loading frequency on damping ratio can be indicated by Fig. 15. The damping ratio increases linearly with the increase of dynamic strain. Moreover, the damping ratio at the loading frequency of 4Hz is close to that at the loading frequency of 6Hz. One reason may contribute to the occurrence of

the phenomena: when the high frequency loading is applied on specimen, there is not sufficient time for glass beads to rearrange, leading to large deformation of specimen.

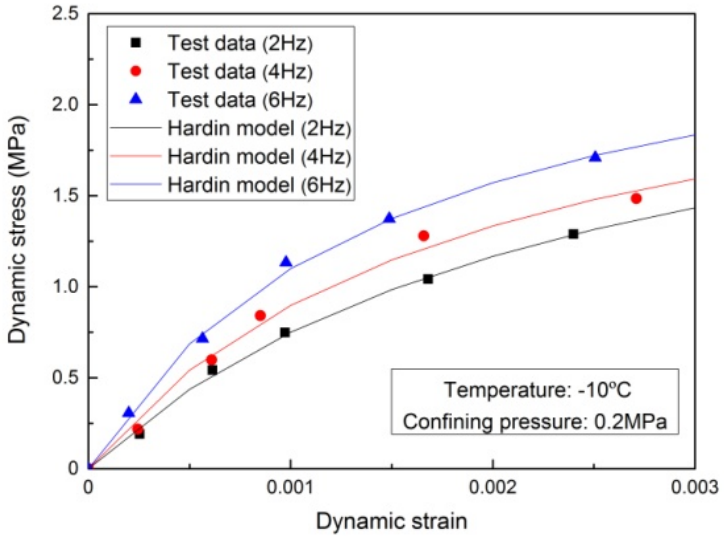


**Figure 13:** Backbone curves under different loading frequencies

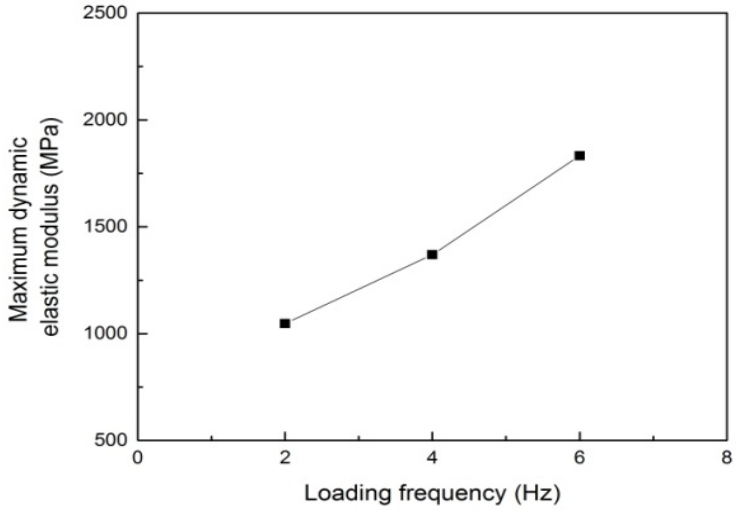


**Figure 14:** The relationship between maximum dynamic elastic modulus and loading frequency.

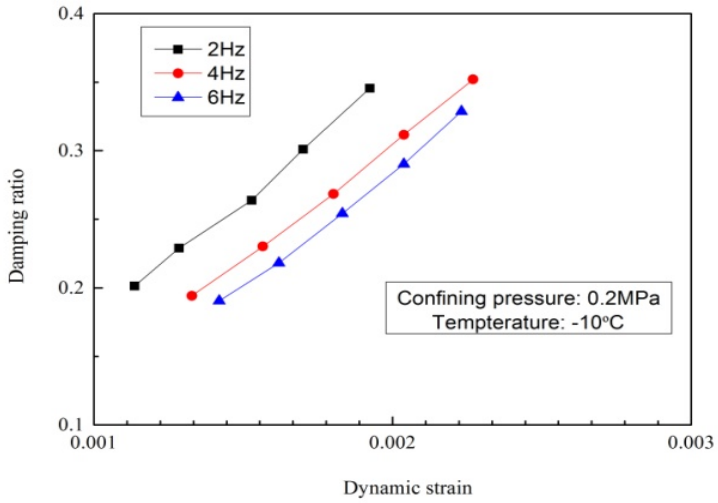


**Figure 15:** Damping ratios under different loading frequencies

*(d) Influence of confining pressure*

The influences of confining pressure on dynamic elastic modulus and damping ratio were analyzed by three tests with different confining pressures (0.1MPa, 0.2MPa and 0.3MPa). In addition, the temperature was -10℃ and the loading frequency was 4Hz. Fig. 16 presents the effect of confining pressure on backbone curve. It indicates that the evolution trend of backbone curves under different confining pressures is consistent and the backbone curve is strongly influenced by confining pressure. Fig. 16 also shows that the dynamic stress increases with the increase of confining pressure for a given dynamic strain. The variation of maximum dynamic elastic modulus versus confining pressure is presented in Fig. 17. The maximum dynamic elastic modulus increases from 1222MPa to 1712MPa as the confining pressure increases from 0.1MPa to 0.3MPa. The effect of confining pressure on damping ratio can be indicated by Fig. 18. It can be seen that the damping ratio is strongly influenced by confining pressure. A general trend that the lower confining pressure is corresponding to the higher damping ratio for a certain dynamic strain can be obtained. It seems that the higher confining pressure leads to the ordered rearrangement of glass beads can account for the phenomena.

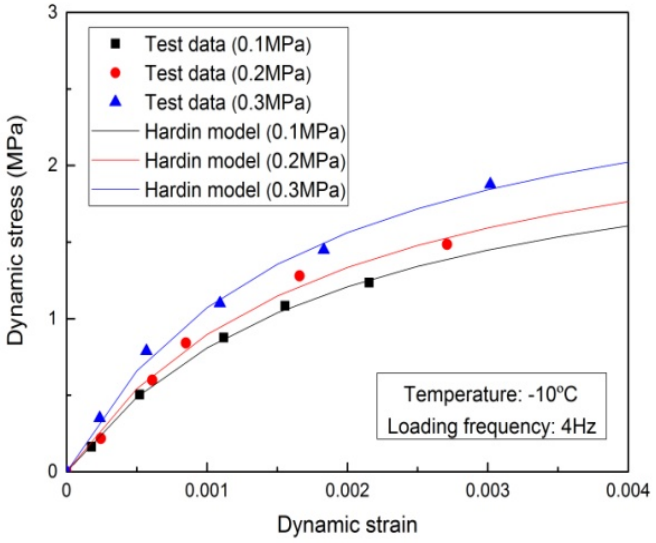


**Figure 16:** Backbone curves under different confining pressures

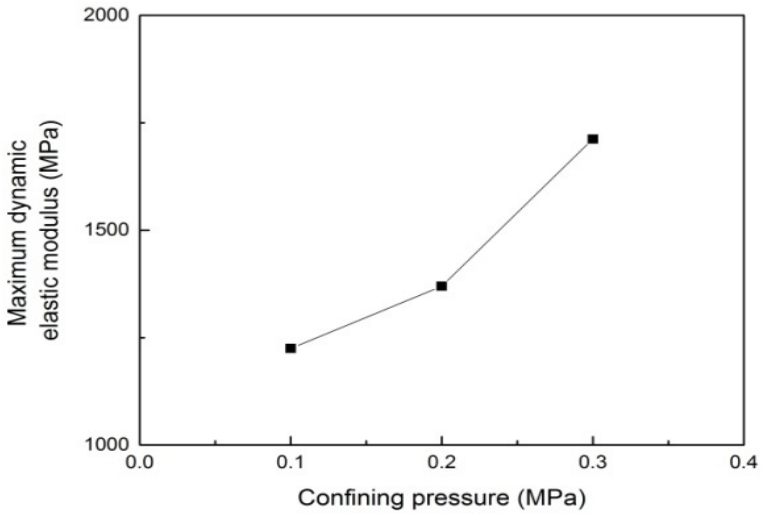


**Figure 17:** The relationship between maximum dynamic elastic modulus and confining pressure.

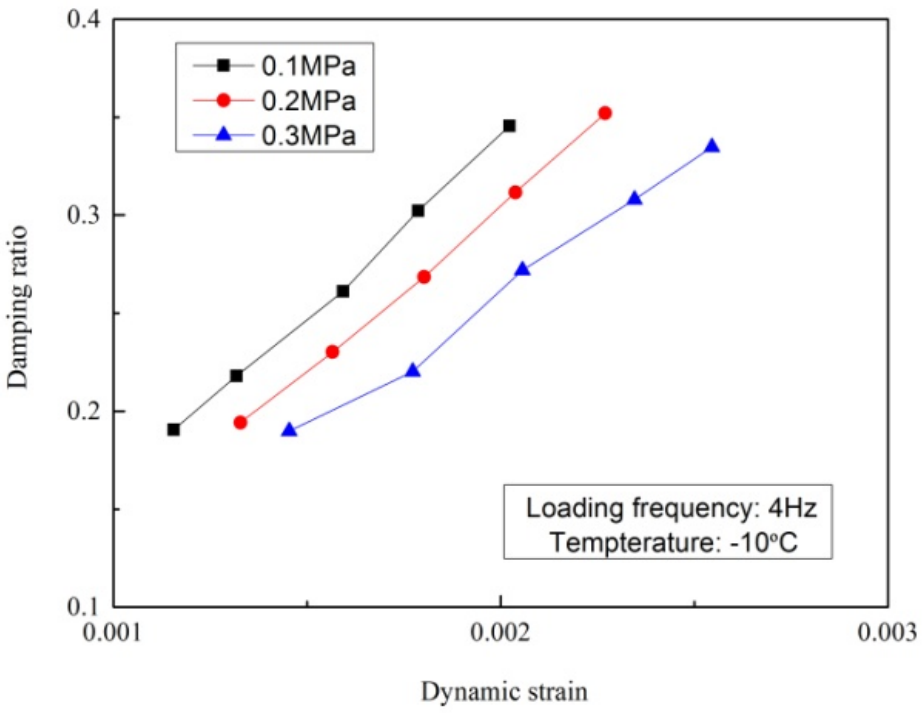


**Figure 18:** Damping ratios under different confining pressures

## CONCLUSIONS

Under low confining pressure (0.1MPa to 0.3MPa) and temperature (-15℃ to -5℃) condition, a series of single-stage cyclic triaxial tests in laboratory were performed to investigate the mechanical properties of ice-rich frozen soil simulated by glass beads subjected to cyclic loading. Based on the test data, the following conclusions can be drawn:

1) It is necessary to take into account the cyclic loading characteristics and the original definition of equivalent linear model for determining the dynamic elastic modulus and damping ratio.

2) In general, temperature has the greatest impact on backbone curve and damping ratio. The maximum dynamic elastic modulus decreases from 2439MPa to 781MPa which means a 68 percent decline as the temperature increases from -15℃ to -5℃. The damping ratio ranges from 0.19 to 0.35.

3) Other influence factors such as confining pressure and loading frequency also have a significant effect on dynamic elastic modulus and damping ratio. The maximum dynamic elastic modulus increases from 1222MPa to 1712MPa as the confining pressure increases from 0.1MPa to 0.3MPa. The damping ratio increases linearly with the increase of dynamic strain. Moreover, the damping ratio at the loading frequency of 4Hz is close to that at the loading frequency of 6Hz.

## ACKNOWLEDGMENTS

Firstly, the authors will thank the people of Heilongjiang Provincial Hydraulic Research Institute of China. Simultaneously, this research was supported by the following agents: National Basic

Research Program of China (Grant No. 2012CB026104), National Natural Science Foundation of China (Grant No. 51174261) and (Grant No. 51078111), and Natural Science Foundation of Heilongjiang Province (No. ZD201218).

# REFERENCES

1. Li, Qionglin., Ling, Xianzhang., Wang Lina., et al. (2013) "Accumulative strain of clays in cold region under long-term low-level repeated cyclic loading Experimental evidence and accumulation model, " *Cold Regions Science and Technology* 94, 45-52.
2. Viklander, Peter. (1998) "Permeability and volume changes in till due to cyclic freeze-thaw, " *Canadian Geotechnical Journal* 35, 471-477.
3. Zhang, Feng. (2012) "Heavy Truck Induced Dynamic Response and Permanent Deformation of Subgrade in Deep Seasonally Frozen Region, " Ph.D, Dissertation, Harbin Institute of Technology.
4. Simonsen, Erik., Janoo Vincent., Isacsson, Ulf. (2002) "Resilient properties of unbound road materials during seasonal frost conditions, " *Journal of Cold Regions Engineering* 16 (1), 28-50.
5. Tuğba, Eskişar., Selim, Altun. (2015) "Assessment of strength development and freeze-thaw performance of cement treated clays at different water contents, " *Cold Regions Science and Technology* 111, 50-59.
6. Qi, Jilin., Vermeer, P.A. (2006) "A review of the influence of freeze-thaw cycles on soil geotechnical properties, " *Permafrost and Periglacial Progress*. 17 (3), 245-252.
7. Wang, Dayan., Ma Wei., Niu Yonghong., et al. (2007) "Effects of cyclic freezing and thawing on mechanical properties of Qinghai-Tibet clay, " *Cold Regions Science and Technology* 48, 34-43.
8. TS, Vinson., RL, Czajkowski. (1978) "Behavior of Frozen Clay under Cyclic Axial Loading, " *Journal of the Geotechnical Engineering Division* 104, 779-800.
9. Ling, Xianzhang., Zhang, Feng. (2015) "Dynamic shear modulus and damping ratio of frozen compacted sand subjected to freeze-thaw cycle under multi-stage cyclic loading, " *Soil Dynamics and Earthquake Engineering* 76, 111-121.
10. Shen, Zhongyan., Zhang, Jiayi. (1997) "Dynamic Strength Characteristics and Failure Criterion of Frozen Silt, " *Journal of Glaciology and Geocryology* 19, 141-148.
11. Xie, Qijun., Zhu, Zhiwu. (2014) "Dynamic stress-strain behavior of frozen soil: Experiments and modeling, " *Cold Regions Science and Technology* 106, 153-160.
12. Gao, Zhihua., Lai, Yuanming. (2010) "Experimental study of characteristics of warm and ice-rich frozen clay under cyclic loading, " *Rock and Soil Mechanics* 31, 1744-1751.
13. Seed, H.B., Wong, R.T., Idriss, I.M., Tokimatsu, K. (1984) "Moduli and damping factors for dynamic analyses of cohesionless soils," Earthquake Engineering Research Center, University of California, Berkeley Report No, pp. 1-37.
14. Seed, H.B., Idriss, I.M. (1970) "Soil moduli and damping factors for dynamic response analyses, Earthquake Engineer Research Center, University of California, Berkeley Report, pp. 1-10.

15. Hardin, B.O., Drmevich, V.P. (1972) "Shear modulus and damping in soils: designing equations and curves," *ASCE Journal of Soil Mechanics and Foundations Division* 98, 667-692.



***Editor's note.***
This paper may be referred to, in other articles, as:

Lingshi An, Xianzhang Ling, Yongchang Geng, Qionglin Li, Feng Zhang: "Mechanical Properties of Ice-Rich Frozen Soil Simulated by Glass Beads Subjected to Cyclic Loading" *Electronic Journal of Geotechnical Engineering*, 2016 (21.16), pp 5293-5309. Available at **ejge.com**.